Available on CMS information server

CMS CR -2018/167

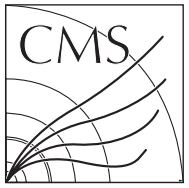

The Compact Muon Solenoid Experiment

Conference Report

Mailing address: CMS CERN, CH-1211 GENEVA 23, Switzerland

20 August 2018 (v3, 14 January 2019)

The performance of the CMS Muon system with data at $\sqrt{s}$ = 13 TeV

Roumyana Mileva Hadjiiska for the CMS Collaboration

Abstract

The muon spectrometer of the CMS experiment is based on three different gaseous detector technologies: Drift Tube (DT) chambers in the barrel, Cathode Strip Chambers (CSC) in the endcaps, and Resistive Plate Chambers (RPC) both in the barrel and endcaps. The performance of the muon system has been studied with LHC proton-proton collision data, collected with the CMS detector, at $\sqrt{s}$ = 13 TeV. The redundancy of the muon detectors ensures correct and reliable muon identification, as well as triggering, in the harsh conditions of high instantaneous luminosity. In this talk, the different components of the muon spectrometer will be described and the performance of the system will be presented in its main aspects.

Presented at *BPU10 The 10th Jubilee Conference of the Balkan Physical Union*

Conference report

14th BPU10: The 10th Jubilee Conference of the Balkan Physical Union
Sofia - Bulgaria
26-30 August 2018

Performance of the CMS Muon system with data at $\sqrt{s}$ =13 TeV

R Hadjiiska,[a,1] **on behalf of the CMS collaboration**

[a] *Bulgarian Academy of Sciences, Inst. for Nucl. Res. and Nucl. Energy, Tzarigradsko shaussee Boulevard 72, BG-1784 Sofia, Bulgaria*

E-mail: roumyana.mileva.hadjiiska@cern.ch

Abstract: The muon spectrometer of the CMS experiment is based on three different gaseous detector technologies: Drift Tube (DT) chambers in the barrel, Cathode Strip Chambers (CSC) in the endcaps, and Resistive Plate Chambers (RPC) both in the barrel and endcaps. The performance of the muon system has been studied with LHC proton-proton collision data, collected with the CMS detector, at $\sqrt{s}$ =13 TeV. The redundancy of the muon detectors ensures correct and reliable muon identification, as well as triggering, in the harsh conditions of high instantaneous luminosity. In this talk, the different components of the muon spectrometer will be described and the performance of the system will be presented in its main aspects.

Keywords: Gaseous detectors, Muon spectrometers, Performance of High Energy Physics Detectors

[1]Corresponding author.

Contents

1 Introduction

The CMS (Compact Muon Solenoid) [1] is a general purpose detector that is used to search for evidence for physics events from and beyond the standard model of particle physics exploring the data collected from proton-proton and heavy ions collisions at LHC (Large Hadron Collider) in CERN. The topologies of a big fraction of the interesting events contain muons in its final states where the muon transverse momentum varies in a large range between a few GeV to $\sim$ 1 TeV. Because of this, a highly performing and redundant muon spectrometer is of crucial importance for muon reconstruction and identification, including p_T measurement, muon charge assignment, and robust muon trigger [2].

2 CMS Muon System

An $R - z$ cross section of a quadrant of the CMS detector is shown on figure 1. The CMS muon system currently exploits three different gaseous detector technologies - Drift Tubes (DT) in the barrel (central) region, Cathode Strip Chambers (CSC) in the endcap (forward) region, and Resistive Plate Chambers (RPC) in both barrel and endcap, covering a pseudorapidity region of $|\eta| < 2.4$. A detailed description of the CMS muon system is available in [3] and in this paper are given only the main layouts of it.

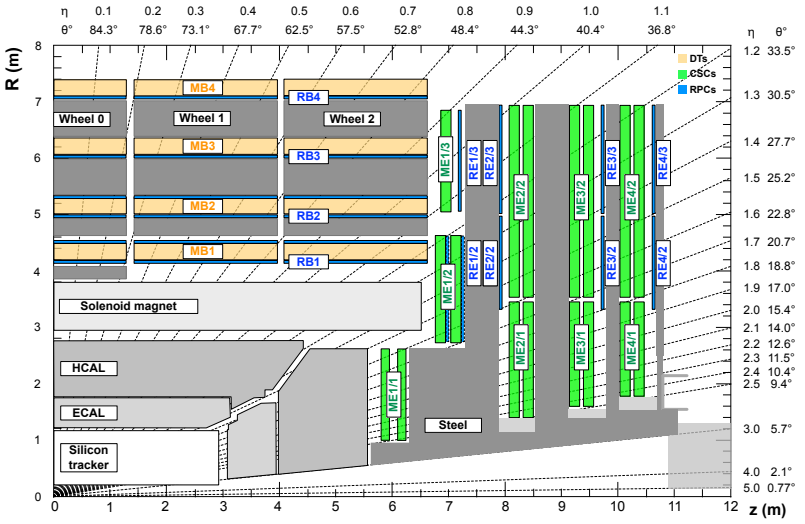

Figure 1. An $R-z$ cross section of a quadrant of the CMS detector. The interaction point is in the lower left corner. The z axis, parallel to the beam, is horizontal and the radius R increases upward. The DT stations are labeled MB (Muon Barrel) and shown in orange, and the CSCs are labeled ME (Muon Endcap) and shown in green. The RPCs are shown in blue and labeled RB in the barrel and RE in the endcaps. The steel flux return disks are shown in gray.

2.1 Drift Tube Chambers (DT)

The Drift Tube Chambers are used as tracking and triggering detectors. As a working gas they use 8515% $ArCO_2$ gas mixture. There are 250 DT chambers distributed among 5 barrel wheels. Each wheel consists of four concentric stations segmented into 12 sectors, where every sector covers $\sim 30^o$ in ϕ. The top sectors in the forth station are equipped with two additional DT chambers. Every DT chamber in the first three stations consists of 12 layers of drift cells forming three super-layers (every super-layer is built of four layer). Two of them are parallel to the beam line and measure the coordinate in the CMS bending plane $r-\phi$. The other one provides information about the z coordinate. The chambers in MB4 have only two $r-\phi$ super-layers. The design resolution is $\sim 250\,\mu$m for reconstructed hits and $\sim 100\,\mu$m for reconstructed segments.

2.2 Cathode Strip Chambers (CSC)

There are 540 Cathode Strips Chambers mounted in the four endcap stations of the muon system. 72 of them have been installed in the outermost disks layers during LS1 (Long Shutdown 1) in order to complete its design layout [4]. The CSCs operate with a 405010%$ArCO_2CF_4$ gas mixture. In rings ME21, 31, and 41, each chamber covers 20^o in ϕ while all other chambers cover 10^o in ϕ. The CSCs have a trapezoidal shape and each chamber is built with 6 layers of anode wires enclosed between cathode planes. The cathodes are segmented in radial strips and provide measurements in the $r-\phi$ plane. The anode wires are orthogonal to the strips and used to measure the radial coordinate. The CSC strip design resolution for single reconstructed hits is expected to be less than $150\,\mu$m.

2.3 Resistive Plate Chambers (RPC)

The CMS RPCs are used mainly as trigger detectors. They are 1056 double gap chambers installed in both the barrel and endcap regions. The two innermost barrel stations are equipped with two RPC layers while the third and fourth have only one RPC layer. In the endcap, RPCs are installed on the second and third ring on every station. During LS1 the fourth stations were completed with additional 144 chambers adding one more layer in order to improve the trigger efficiency. The CMS RPCs have Bakelite plates with a bulk resistivity in the range of $10^{10} - 10^{11}$ Ω·cm. The chambers work in a avalanche mode and the intrinsic time resolution is ≈ 2 ns [5]. The working gas mixture is composed by 95.2% Freon ($C_2H_2F_4$), 4.5% Isobutane (iC_4H_{10}), and 0.3% SF_6.

3 Performance of the muon detectors during LHC Run-2

The first run of the LHC data taking (Run-1) lasted from 2010 till 2012. With the start of Run-2 in 2015, the center of mass energy increases from 8 to 13 TeV and the instantaneous luminosity reaches values more than 2×10^{34} cm^{-2}s^{-1}. The average number of the pile-up events during a proton-proton collision is ∼ 38 [6]. Keeping the best performance of the muon detectors in a harsh condition requires permanent monitoring of the main detector parameters, such as hit and trigger efficiency and spatial resolution. They have been studied with proton-proton collision data. As a main method for efficiency calculation the Tag-and-Probe ($T\&P$) technique has been used [7]. Wherever needed, other techniques have also been applied..

3.1 Hit and segment reconstruction efficiency

The DT hit efficiency measured with proton-proton collision data at $\sqrt{s}$ =13 TeV is shown in figure 2. It was defined and measured as the ratio between the number of detected and expected hits. A probe set of track segments reconstructed in both ϕ and θ views has been used to determine the positions of the expected hits. At least 7 (for ϕ segments) or 3 (for η) hits were required to be associated to a segment in layers other than the one under study. The intersection of such a high quality track segment with the layer under study determines the expected position. The cell was considered efficient if a detected hit was found within it. To avoid any bias, segments crossing known dead cells were rejected. As can be seen from the plot, the DT hit efficiency is high, with an average value of more than 97% for almost of the chambers.

The RPC hit efficiency has been studied with the $T\&P$ method. Oppositely charged muon pairs have been selected from data that passed the single-muon trigger. The tag muon was required to pass tight identification and isolation criteria. Another muon (probe) is selected to pass the tracker track quality requirements and to form a $Z \rightarrow \mu\mu$ resonance pair with the tagged one. The RPC hit efficiency for all the chambers is shown in figure 3. The left plot shows a comparison between the efficiency distributions for the barrel chambers during the three years of the Run-2 data taking and the right plot relates to the endcap chambers. As can be seen from the plot the RPC hit efficiency is higher than 95%, better than the CMS requirements, and has been stable over the years. The small

differences are caused by variations of the working gas mixture. There is a small fraction (~ 5% out of total 1056) of chambers with known problems and efficiency lower than 70%. These are mainly the chambers switched OFF in order to reduce gas leaks.

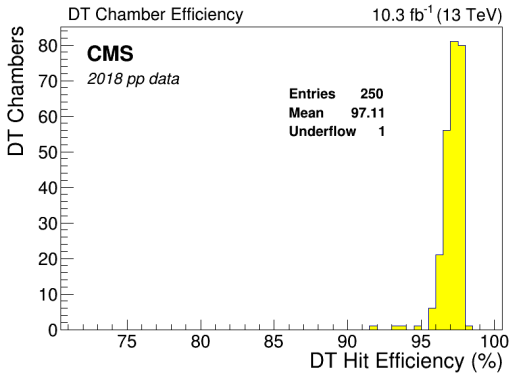

Figure 2. DT hit efficiency distribution: 1 entry per chamber. Dead channels are not taken into account.

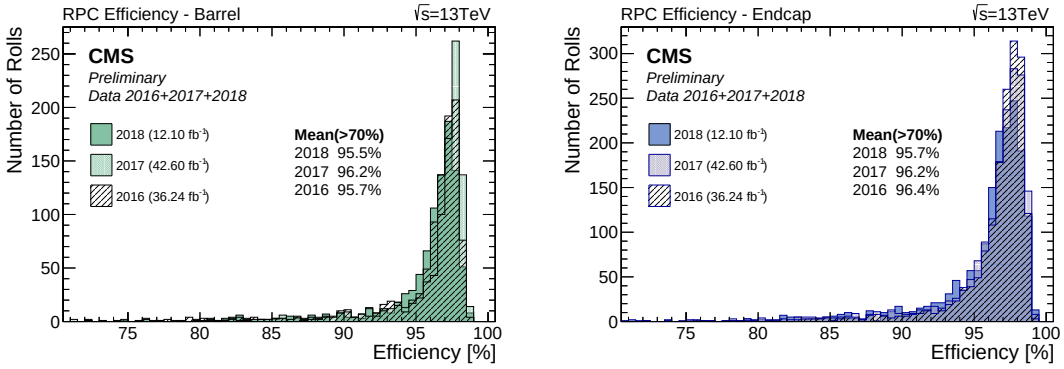

(a) (b)

Figure 3. RPC overall efficiency distribution in the barrel (a) and endcap (b).

The DTs and CSCs are multilayer detectors. A segment in a CSC or DT is a straight-line track segment reconstructed from the hits on particular layers of the CSC in the endcap and DT in the barrel. The segments are used as seeds for the full CMS muon track reconstruction algorithm, in combination with tracks reconstructed in the Silicon Tracker, in both the CMS High-Level Trigger (HLT) and CMS offline muon reconstruction. The segment efficiencies are calculated with the $T\&P$ method. More details about the kinematic and selection criteria to the tagged and probed muons are given in [2]. For the DT segment efficiency calculation, the inner components of probes that passed the selection criteria have been propagated to each station of the DT detector and checked to have segments matched in ≥ 1 muon stations different from the one under study. A DT chamber crossed by a probe track is considered efficient if a reconstructed segment is found within 15 cm distance of the extrapolated track in the $R-\phi$ plane. For the CSC segment efficiency calculation the probe track is projected into the CSC system and a matching segment is searched for in each CSC the track traverses. To reduce backgrounds and ensure that the probe actually enters the CSC under consideration, compatible hits are also required in a downstream CSC. The DT segment efficiency

as a function of the pseudorapidity η is given in figure 4. Since here the efficiency is integrated over ϕ, the presence of gaps between sectors has the effect of lowering the efficiency observed within the η acceptance. Station 4 does not have ϕ gaps between most sectors, therefore its efficiency, within the η acceptance, is higher than the other stations. Figure 5 shows the CSC segment efficiency of each Cathode Strip Chamber. There are a few (out of the total 540) chambers with known inefficiency usually due to one or more failed electronics boards that cannot be repaired without major intervention and dismantling of the system. There are also occasional temporary failures of electronics boards, lasting from periods of hours to days, which can be recovered without major intervention. Both contribute to lowered segment efficiency. Nevertheless the segment efficiency of the muon system is high and above 95%.

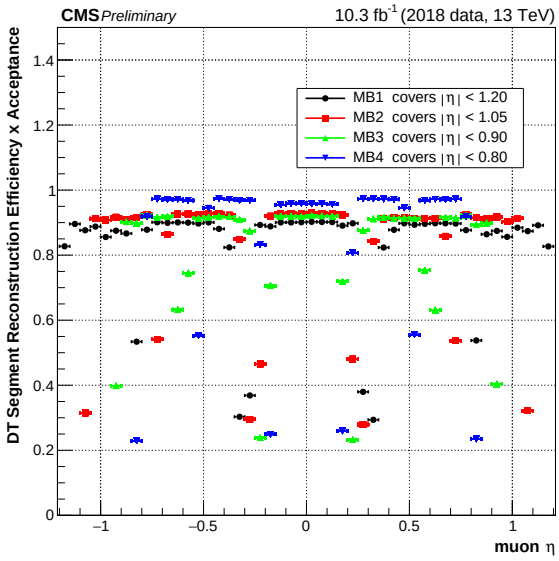

Figure 4. Segment Reconstruction Efficiency in the four muon barrel (MB) stations, computed within the full solid angle, as a function of the probe's η. Variations are dominated by the presence of gaps between wheels, not covered by drift tube chambers.

3.2 Space Resolution

The single hit resolution for the DTs is shown in figure 6(a)and for the CSCs in 6(b). The CSC spatial resolution per station measured for all chamber types in 2017 and early 2018 is shown in figure 6(b). It has been estimated by fitting a Gaussian to the residual distributions for every ring. The residuals were calculated as the difference between the positions of the reconstructed hit in a given layer in a chamber and the segment reconstructed in all the other layers in the same chamber. Depending on the chamber type, the CSC spatial resolution varies from 45 μm for the first ring of the first station and 145 μm for the last station, which meet the design requirements. A comparison between 2017 and 2018 data shows no change with respect to the previous year. A similar approach has been used to compute the DT single hit resolution, measuring the widths of the distributions of the distances between every reconstructed hit and the fitted segment it belongs to. Hits reconstructed

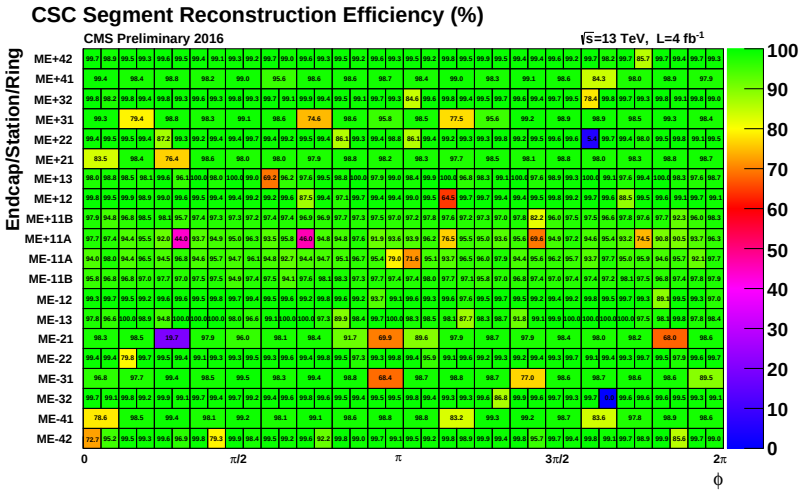

Figure 5. The efficiency (in %) of each Cathode Strip Chamber in the CMS endcap muon detector to provide a reconstructed muon track segment.

within the same station of the same wheel were added together. In order to take into account the geometrical differences ϕ (measuring in $R-\phi$ plane) and θ SL ($R-Z$ plane) super-layers (SL) are kept separately. In Wheel 0 ($W0$) most of the tracks coming from the interaction points are normal to all layers and the resolution is the same for both the ϕ and θ SL. Going from z=0 towards the forward regions, the inclination angle increases the track path within the tube along the wire direction in ϕ SL, thus increasing the ionization charge and improving the resolution. There is no θ SL in the last fourth barrel station (MB4) and no position information is available in the direction parallel to the wires. Because of this, no corrections for the signal propagation along the wire was applied to this station, which is the reason for relatively poorer resolution compared to the first three stations.

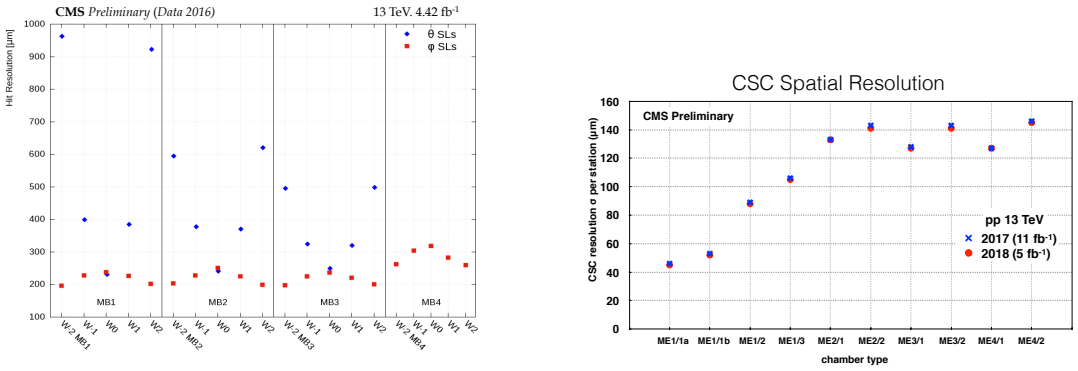

(a) (b)

Figure 6. Single hit resolution for DT (a) and CSC (b) stations measured with proton-proton collision data in Run-2. MB depicts the muon barrel station numbers while W corresponds to the wheels. ME relate to the muon endcap stations. Statistical uncertainties from the fits are negligible, and systematic uncertainties $\sim 1-2\,\mu$m dominate.

By design the RPCs are used mainly as trigger detectors. Nevertheless they contribute and complement the information about the ϕ space measurements and evaluation of the bending angle. The RPC single hit resolution has been studied with the help of the Segment extrapolation method [8] where the segments built in the nearest DT or CSC chamber have been extrapolated to the plane of the RPC under study. Gaussian fits to the distributions of the differences between the positions of the extrapolated and reconstructed hits have been performed. The obtained widths depend on the strip pitch and vary between 0.93 cm for the innermost stations and 1.4 cm for the outermost. The Cluster size (CLS) for RPCs is defined as the number of adjacent fired strips in a given time window of 25 ns. The position of the reconstructed hit is determined in the gravity center of such clusters and thus the single hit resolution depends on the CLS. In order to reject possible noisy events, which may affect the ϕ bending angle estimations, the hits with $CLS > 3$ are cut on the trigger level. As can be seen from figure 7, the average CLS is ~ 2 and it is kept below the trigger requirements.

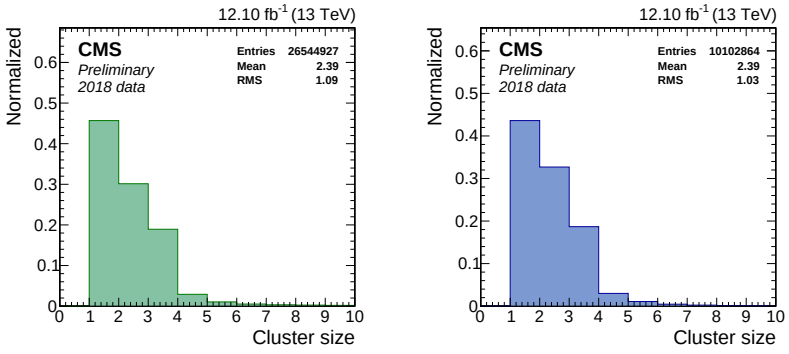

(a) (b)

Figure 7. RPC cluster size distribution in the barrel (a) and endcap (b).

3.3 Muon Level1 Trigger Upgrade

To cope with the new Run-2 conditions and reduce the increased event rate while maintaining a high efficiency in the same time, the first level of the trigger system (L1 trigger) has been upgraded. The muon L1 upgrade began in 2016 moving from a muon detector-based scheme (DT, RPC, and CSC) to a geometry-based system. The new trigger logic combines the information – hits and segments from all muon detectors and sends it to three different track finders – BMTF (Barrel Muon Track Finder), OMTF (Overlap Muon Track Finder) and EMTF (Endcap Muon Track Finder). BMTF uses information from DTs and RPCs and covers the pseudorapidity region up to $|\eta| \leq 0.83$. In the overlap region, $0.83 < |\eta| \leq 1.24$, OMTF combines the information from all three muon subsystems – DT, RPC and CSC. In the region with $|\eta| < 1.24$, EMTF uses information from the CSCs and RPCs [9]. The three track finders send muons to the global trigger (μGMT) which sorts and cancels duplicate muons. The upgrade system reduces the trigger rate roughly by a factor of 2 and slightly increases the overall trigger efficiency [10, 11]. Figure 8(a) shows the rates of $L1$ muons passing the threshold from 25 GeV as measured in 2017 data compared with the emulated legacy trigger (2015) as a function of η. As can be seen from the plot, the rate reduction reaches $\sim$ 80% in the very forward regions. Figure 8(b) shows the efficiency of all muon track finders measured with

proton-proton collision data in 2018 as a function of the muon p_T. The efficiency is measured to be greater than 90% for all track finders for the muons with $p_T > 22$ GeV, which is the most common single-muon trigger threshold used in CMS analyses. The upgrade was completed in 2017, with the addition of combined *DT+RPC* trigger primitives from the TwinMux [12] system in the barrel region, and RPC primitives from CPPF (Concentrator Pre-Processor and Fan-out) in the endcap. Additional RPC layers on the first and second muon barrel stations allow the construction of "RPC pseudo-segments" that improve the trigger efficiency for these stations. Such an effect is shown in figure 8(c), where the DT Local Trigger Efficiency in the four MB stations is plotted as a function of the probe's η. Variations are dominated by the presence of gaps between wheels not covered by drift tube chambers. Far from these gaps, the efficiency is near 99% for MB1 and MB2. It is 95 – 96% for MB3 and MB4, where the RPC-only primitives are not implemented [13].

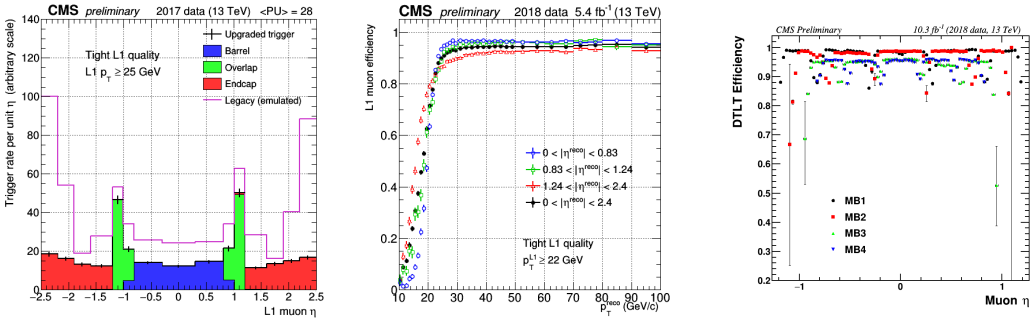

(a) (b) (c)

Figure 8. (a): The distributions of $L1$ muons with $p_T > 25$ GeV as a function of η built by the three track finders in the upgraded L1 muon trigger (2017), and compared with the emulated legacy trigger (2015), in arbitrary units. (b): the efficiency for all muon track finders vs muon probe's p_T. (c): DT Local Trigger Efficiency in the four MB stations, computed within the full solid angle, as a function of the probe's η.

4 Conclusion

The main detector parameters of the CMS muon system have been studied with proton-proton collision data at $\sqrt{s}$= 13 TeV (almost twice the amount compared to Run-1) and instantaneous luminosity reaching more than 10^{34} cm^{-1} s^{-1} (approaching the design luminosity of 5×10^{34} cm^{-1} s^{-1}) during LHC Run-2. The new detection layers added in LS1 (Long Shutdown 1) and the trigger algorithm changes improved the redundancy of the system. Thus the efficiencies for muon measuring and triggering have been kept within the designed requirements and comparable with the performance during Run-1. Thanks to the stable operation of the entire CMS detector, and in particular the muon system, more than 134.4 fb^{-1} have been collected during Run-2, providing valuable data for physics analyses and searches.

Acknowledgments

We would like to thank especially all our colleagues from the CMS muon group and L1 muon trigger group for their dedicated work to keep the stable performance of the system. We congratulate our colleagues in the CERN accelerator departments for the excellent performance of the LHC and thank the technical and administrative staffs at CERN and at other CMS institutes for their contributions to the success of the CMS effort. In addition, we gratefully acknowledge the computing centres and personnel of the Worldwide LHC Computing Grid for delivering so effectively the computing infrastructure essential to our analyses. Finally, we acknowledge the enduring support for the construction and operation of the LHC and the CMS detector provided by the following funding agencies: BMBWF and FWF (Austria); FNRS and FWO (Belgium); CNPq, CAPES, FAPERJ, FAPERGS, and FAPESP (Brazil); MES (Bulgaria); CERN; CAS, MoST, and NSFC (China); COLCIENCIAS (Colombia); MSES and CSF (Croatia); RPF (Cyprus); SENESCYT (Ecuador); MoER, ERC IUT, and ERDF (Estonia); Academy of Finland, MEC, and HIP (Finland); CEA and CNRS/IN2P3 (France); BMBF, DFG, and HGF (Germany); GSRT (Greece); NKFIA (Hungary); DAE and DST (India); IPM (Iran); SFI (Ireland); INFN (Italy); MSIP and NRF (Republic of Korea); MES (Latvia); LAS (Lithuania); MOE and UM (Malaysia); BUAP, CINVESTAV, CONACYT, LNS, SEP, and UASLP-FAI (Mexico); MOS (Montenegro); MBIE (New Zealand); PAEC (Pakistan); MSHE and NSC (Poland); FCT (Portugal); JINR (Dubna); MON, RosAtom, RAS, RFBR, and NRC KI (Russia); MESTD (Serbia); SEIDI, CPAN, PCTI, and FEDER (Spain); MOSTR (Sri Lanka); Swiss Funding Agencies (Switzerland); MST (Taipei); ThEPCenter, IPST, STAR, and NSTDA (Thailand); TUBITAK and TAEK (Turkey); NASU and SFFR (Ukraine); STFC (United Kingdom); DOE and NSF (USA).

References

[1] CMS Collaboration, *The CMS experiment at the CERN LHC,* J. Instrum. 3 (2008) S08004.

[2] CMS Collaboration, *Performance of the CMS muon detector and muon reconstruction with proton-proton collisions at* $\sqrt{s}$=13TeV, 2018 JINST 13 P06015, [arXiv:1804.04528].

[3] CMS Collaboration, *The CMS muon project*: *Technical Design Report.* 1997. CERN-LHCC-97-032, CMS-TDR-003.

[4] C. Battilana et al. [CMS Collaboration], *The CMS muon system: status and upgrades for LHC Run-*2 *and performance of muon reconstruction with* 13 *TeV data,* 2017 JINST 12 C01048.

[5] M. Abbrescia et al., *Beam test results on double-gap resistive plate chambers proposed for CMS experiment*, *Nucl. Instr. Meth.* **A 414** (1998) 135–148

[6] *CMS Luminosity - Public Results*

[7] CMS Collaboration, *Performance of CMS muon reconstruction in pp collision events at* $\sqrt{s}$=7TeV, 2012 JINST 7 P10002, [arXiv:1206.4071].

[8] C. Camilo [CMS Collaboration], *The CMS Resistive Plate Chambers system-detector performance during 2011,* WSPC (2012), 10.1142/9789814405072-0068.

[9] J. Fulcher, J. Lingemann, D. Rabady, T. Reis, S. Hannes [CMS Collaboration], *The New Global Muon Trigger of the CMS Experiment,* IEEE Trans. Nucl. Sci. 64 (2017) 1467-1473.

[10] CMS Collaboration, Level - 1 muon trigger performance in 2017 data and comparison with the legacy muon trigger system, *CERN-CMS-DP-2016-074*

[11] CMS Collaboration, Level - 1 muon trigger performance, *CERN-CMS-DP-2018-044*

[12] A. Triossi et al. [CMS Collaboration], *The CMS Barrel Muon trigger upgrade*, 2017 JINST 12, C01095.

[13] CMS Collaboration, Performance of CMS muon detectors in 2018 Collision Runs, *CERN-CMS-DP-2018-047*